DOI: https://doi.org/10.37434/tpwj2023.12.05

# INVESTIGATIONS OF THE QUALITY OF METAL OF HIGH-MANGANESE STEEL ALLOYED BY ALUMINIUM AND CHROMIUM AFTER ELECTROSLAG REMELTING

**V.A. Zaitsev, Yu.V. Kostetskyi, G.O. Polishko, V.A. Kostin, V.P. Petrenko, E.O. Pedchenko**

E.O. Paton Electric Welding Institute of the NASU
11 Kazymyr Malevych Str., 03150, Kyiv, Ukraine

**ABSTRACT**

The paper presents the results of investigation of the influence of electroslag remelting on the properties of metal of ingots of high-manganese steel, alloyed by aluminium and chromium. Features of structure formation in high-alloy manganese steels are considered. These steels demonstrate ductility and lower density, alongside strength, and are difficult for pouring alloys, prone to hot cracking, formation of a coarse structure and development of macro- and microliquation. Studies have been performed, which confirm the conclusions that steels of this type require a thorough control of solidification conditions. Obtained results illustrate a significant influence of the cooling rate on cracking, manganese and aluminium segregation and parameters of the alloy dendritic structure. Electroslag remelting resulted in improvement of the structure and led to reduction of the size of nonmetallic inclusions in the studied metal without any significant changes in Mn, Al and Cr content, which is one of the conditions for producing large-sized homogeneous ingots. Metallographic examinations showed that the microstructure of all the studied steel specimens is characteristic for austenitic steel with dendritic crystal growth. Dendritic structure in the metal of ESR ingot is homogeneous, distances between the first and second order axes in the ingot middle and upper parts are equal to 136.6–146.5 and 60.54–8.92 μm, respectively. Completing formation of the required final microstructure of the studied steel takes place after further heat and thermodeformational treatment. ESR of cast billets allows reaching the required level of metal homogeneity and specified level of properties with a smaller number of stages and duration of thermomechanical treatment, and reducing resource consumption.

**KEYWORDS:** high-strength lightweight steel, ingot, electroslag remelting, microstructure, liquation, phase composition

## INTRODUCTION

The development of modern industry involves not only the development and application of new structural materials, but also the creation of effective technologies for their production. Over the past few decades, many studies have been carried out, devoted to the investigation of the properties of Fe–Mn–Al–C steels [1–5] from the point of view of the possibility of their application in the power, chemical, mining and defence industries, infrastructure construction and transport engineering. For some period of time, Fe–Mn–Al–C steels were considered as a possible replacement for conventional chrome-nickel stainless steels [5]. In the 80s and 90s of the last century, the influence of their corrosion resistance, weldability, oxidation resistance, effect of temperature, chemical composition and microstructure on mechanical properties was actively investigated [4, 5]. One of the most important results of these studies was the awareness and understanding of the relationship between deformation mechanisms and mechanical properties, which attracted the attention of the academic community and ensured rapid progress in the further development and application of Fe–Mn–Al–C steels in the automotive industry. At present, research groups around the world are making efforts for further study of Fe–Mn–Al–C steels to make them more accessible and expand the range of possible applications.

Since the beginning of the 2000s, considerable attention has been paid to the study of Fe–Mn–Al–C steels with reduced density, that were intended for the application in various structures [3–5]. These steels may contain 3–30 % Mn, 3–12 % A1, 0.1–1.5 % C and are distinguished by a unique set of mechanical properties with a yield strength of 0.4–1.0 GPa, a tensile strength of 0.6–2.0 GPa and a relative elongation of 30–100 % [6–9]. Aluminium in the alloy composition provides reduction in the metal density. Each additional percent of aluminium results in a decrease in the metal density by approximately 1.3 %, as well as a decrease in the modulus of elasticity by 2 % and an increase in strength by 40 MPa [6, 10, 11]. Steels of this system with an aluminium content of more than 6 % were allocated to a new class of high-strength lightweight steels (low-density/lightweight steels).

Depending on the chemical composition, high-strength lightweight Fe–Mn–Al–C steels can have an austenitic, ferritic or double (duplex) matrix consisting of ferrite and austenite [4, 10]. Due to the presence of nanosized κ-carbides in the austenite matrix, these alloys show both excellent strength and ductility [4, 5]. Initially, it was assumed that κ-carbides worsen ductility, and to suppress their formation, it was proposed to add boron, titanium and niobium to the

composition of the alloy [9, 12]. However, later it was recognized, that in case of optimizing the morphology, size and distribution of κ-carbides, they may simultaneously improve both strength and ductility [9, 13]. Usually, coarse intercrystalline κ-carbides are undesirable, while intragranular nano-sized κ-carbides contribute to the improvement of mechanical properties [14]. The contribution of nanosized κ-carbides to improvement in the yield strength of steel 1.78 times exceeds the effect of strengthening with dissolved aluminium.

Over the past two decades, new grades of high-strength lightweight steels with an austenitic matrix have been developed, which combine high strength with excellent ductility [2, 6, 7] and are aimed at the needs of the automotive industry.

Austenitic high-strength lightweight steels usually contain 12–30 % of manganese, 0.6–2.0 % of carbon and 5–12 % of aluminium [5, 15, 16]. Their phase structure consists mainly of an austenitic matrix with traces of ferrite, κ-carbides and β-Mn phase. At hot deformation temperatures, these steels have practically one austenitic phase. In the cast state, they show a dendritic microstructure and a tendency to liquation due to a significant content of alloying elements. Slow cooling of these steels leads to the formation of sources of the ferritic phase and coarse κ-carbides mainly along the boundaries of austenitic grains [9, 14]. To reduce micro-inhomogeneities, homogenization is performed with exposure at a temperature of 1100–1250 °C for the required time. The recrystallized microstructure usually contains equiaxial austenitic grains with annealing twins [5]. To avoid precipitation of coarse κ-carbides, these steels are quenched in water at a temperature of 900–1100 °C. During the aging of austenitic Fe–Mn–Al–C steels in the temperature range of 500–900 °C, two types of κ-carbides can also form — intergranular and intragranular [8]. As was mentioned above, the morphology of these carbides significantly affects the properties of steel. In general, these steels show a good combination of strength (600–1700 MPa) and ductility (up to 85 %) [3, 17].

High-strength lightweight austenitic duplex steels may contain 18–28 % Mn, 9–12 % A1 and 0.7–1.2 % C [5]. At temperatures of hot deformation, such steel consists mainly of austenite and a smaller amount of ferritic phase. Due to the significant content of manganese and aluminium, the austenitic phase is quite stable. At room temperature, these steels usually have a stable austenitic phase as a matrix one with precipitations of nanosized κ-carbides dispersed in it (less than 10 vol.%), as well as a small amount of ferritic phase (5–15 vol.%). Steels of this type are a variety of multiphase steels and are known as Triplex steels [6]. They have much better tensile properties than low-density ferritic steels [17].

As research has shown, the cold working of Fe–Mn–Al–C alloys deteriorates significantly with an increase in the aluminium content by more than 10 wt.% due to the propagation of brittleness [9]. Accordingly, the majority of studies of lightweight Fe–Mn–Al–C steels are limited to the compositions with the content of aluminium from 5 to 10 wt.% [6, 18–23]. By the way, it turned out that the addition of Cr can significantly improve the cold working even at a high content of aluminium and carbon [19]. Thus, for example, with the addition of chromium, Fe–20–Mn–13Al–1.3C–5Cr steel was produced with a density of 6430 $kg \cdot m^{-3}$ (a decrease in density is 18.3 %), a yield strength of 915 MPa, a tensile strength of 1140 MPa, and a total elongation of 22 % during uniaxial tensile tests performed at room temperature with a strain rate of $3.3 \cdot 10^{-4} \cdot s^{-1}$. Without the addition of chromium, Fe–20Mn–12Al–l.5C steel has a typical complex microstructure, which mainly consists of austenite with fine dispersed intragranular κ-carbides in it, a small fraction of ferrite and coarse intergranular κ-carbides. It is assumed that Cr, which is a carbide-forming element, suppresses the formation of intergranular κ-carbides and increases the amount of carbon in the austenitic phase.

Thus, acquiring the necessary set of properties by high-strength lightweight Fe–Mn–Al–C steels is determined by the complex relationship between the chemical composition and the micro- and macrostructures formed in the process of solidification of the alloy and during the subsequent heat and thermomechanical treatment. The production of these steels will require compliance with a high culture of production with precise technological control and the introduction of new technologies. As a result, despite the favourable market prospects, the deployment of large-scale commercial production of high-strength lightweight Fe–Mn–Al–C steels is hindered by a number of technical and technological problems that occur at almost all stages of the production process, which makes it quite expensive so far.

High-alloy Fe–Mn–Al–C steels, like other high-manganese steels, are complex alloys for pouring, prone to hot cracking, formation of a rough structure and development of macro- and microliquation [20–24]. A high content of alloying elements significantly affects the nature of the crystallization process, contributes to the development of liquation processes and heterogeneity of the resulting structures. For example, a study of an ingot of medium-manganese steel Fe–5Mn–1.5Al showed that the content of manganese in the central volumes of the ingot is greater than in

the surface volumes, while aluminium shows the opposite tendency to macrosegregation [25]. Studies of the homogeneity of the distribution of impurities at the microlevel in the austenitic steel with a high manganese content showed that, depending on the conditions of crystallization due to the development of liquation, the difference in the content of manganese in different structures can reach 2–7 wt.%, and carbon — 0.06–0.3 wt.% [26]. Against the background of strong liquation, in steels with a complex structure, phases may even form that are not predicted by the equilibrium phase diagram [24]. The liquidation of alloy components and related structural inhomogeneities affect the distribution of mechanical properties, corrosion resistance, efficiency and results of heat and mechanical treatments.

As is shown by special studies, the cooling and the associated solidification rates significantly affect the parameters of the primary structure of the metal at the macro- and microlevels, as well as the degree of segregation of the alloy components, which is predetermined by their different solubility in the formed structures [27, 28]. An increase in the solidification rate helps to obtain a more uniform structure [22, 23], but it is practically impossible to ensure the required cooling rate simultaneously over the entire cross-section of the ingot. In this regard, new and improved continuous pouring technologies were developed and implemented for the production of Fe–Mn–Al–C steel sheets [29, 30]. However, such a solution is not universal, as certain products require pouring of steel into ingots. In this case, before further thermomechanical treatment, it is advisable to subject the produced ingots to the process of electroslag remelting (ESR), which improves the crystalline structure and chemical homogeneity of the cast metal [29, 31]. ESR is widely used in the production of special steels and superalloys to produce ingots that are more pure in terms of nonmetallic inclusions, with minimized macrosegregation and a more uniform microstructure, which allows achieving the required final level of metal homogeneity and a defined level of properties with fewer stages of thermomechanical treatment, reducing time and energy.

This work presents the results of the study of the structure and properties of high-strength lightweight steel (25–28 % Mn, ≤ 3 % Si, 9–11 % Al, 5–6 % Cr, 1.8 % C) in the cast state after pouring into ingots and after the next electroslag remelting in order to determine the effect of remelting on the metal quality.

## RESEARCH PROCEDURE

Melting of the experimental metal was carried out in an induction crucible melting furnace with a subsequent pouring into ingots, which were furtheron used as consumable electrodes during electroslag remelting. For melting of experimental steel, the crucible lining of the induction furnace with a setting of 60 kg was made of a mixture of alumina and magnesite, taken in a ratio of 75/25. Casting moulds to produce castings with a diameter of 0.08 m and a length of up to 0.7 m were made from a sand moulding mixture. To reduce the oxidizing effect of the atmosphere during melting, a layer of protective flux was created on the surface of the liquid metal in the crucible of the induction furnace.

Electroslag remelting of the experimental metal was carried out in an ESR furnace of P-951 type with a current-conducting mould with an inner diameter of 0.18 m and a two-circuit power supply. In order to reduce the loss of alloying components with the oxidation during remelting, over the slag surface in the mould, the partial pressure of oxygen was reduced by blowing argon into the space above the slag through a circumferential distributor pipe. Remelting was carried out with the use of ANF-29 flux. During remelting, a stable electrical mode and a minimal immersion of the electrode were maintained. At the same time, the electric power was equally distributed between the electrode and the current-conducting section of the mould. The filling factor of the mould during remelting was 0.2.

Specimens for chemical analysis and metallographic examinations were cut out from the produced castings and ESR ingot. The content of leading alloying elements in the casting and ingot metal after electroslag remelting is presented in Table 1.

The study of the microstructure of the investigated steel in the cast state and after electroslag remelting was carried out in the Neophot-32 optical microscope, equipped with a digital photography attachment. Images were registered using the QuickPhoto computer program. Digital images were processed using the Atlas program at magnifications of 25–500 times in a light field. The study of the results of the process of

**Table 1.** Content of leading alloying elements in the investigated metal, wt.%

| Specimen | | Al | Si | Cr | Mn |
|---|---|---|---|---|---|
| Cast metal | | 9.96 | 0.38 | 6.10 | 28.45 |
| ESR ingot | Middle of the height | 10.79 | 2.66 | 5.77 | 25.70 |
| | Main part | 10.67 | 1.12 | 6.27 | 28.10 |

crystallization and dispersion of the dendritic structure of the cast metal was carried out by the method of measurement of the distance between the dendrite branches of the first and second order using the Tescan computer program.

The study of the local chemical composition, distribution and composition of phases, distribution of chemical elements, chemical heterogeneity over the section area, morphology and chemical composition of nonmetallic inclusions (NI), as well as obtaining images of the object over a wide range of magnifications in secondary and scattered electrons were carried out using the analytical complex, which is composed of JSM-35CF electron microscope of JEOL Company (Japan) and INCA Energy-350 X-ray spectrometer with dispersion on the energy of X-ray quanta of Oxford Instruments Company (UK). In the work, SEI mode (secondary electrons image) was used to study the morphology and chemical composition of nonmetallic inclusions, as well as building of concentration maps for element distribution. The experiments were performed at an accelerating voltage of 20 kV and at a magnification from 200 to 10000. The elemental analysis was performed in the range from B to U.

According to morphological features and chemical composition, based on the energy dispersion spectral analysis, the inclusions were distributed into types (elemental composition) and their sizes were determined. The results of NI analysis were processed using a special program for quantitative distribution of phases and inclusions (INCA Feature). All results are presented in weight percentages.

Durometric studies were conducted in the durometer Leco-M400. The measurements of Vickers integral hardness were carried out at a load of 50 g.

## RESULTS OF METALLOGRAPHIC EXAMINATIONS OF METAL IN THE CAST STATE

Metallographic examinations of specimens of the studied metal in the cast state were carried out in the cross-section in the areas in the central part of the ingot and near the surface.

The study of the structure and distribution of nonmetallic inclusions was carried out on the sections without etching. Analysis of the obtained results showed that it is possible to clearly separate the phase components in the metal structure: of dark (spectrum 1) and two types of light (spectra 2, 4) colours (Figure 1). The matrix has a light colour and has in its chemical composition: 14 wt.% Al, 0.6 wt.% Si, 5 wt.% Cr, 25 wt.% Mn. In the dark component, an increased content of Mn to 34 wt.% and Cr to 8.12 wt.% is observed.

Analysis of the distribution of dispersed NI showed that they are uniformly located in the matrix, have a predominantly regular globular shape, and their size does not exceed 3 μm in the matrix (Figure 2, spectra 1, 2). It is established that the chemical composition of the inclusion is aluminium oxynitride ($Al_2(O, N)_3$) with a slight content of magnesium impurity (up to 1 %).

The metal structure after etching has a similar appearance with the structure, which is observed on non-etched specimens. After etching of the experimental specimens, eutectic precipitations are clearly revealed on them. The structure of the experimental metal is two-phase: austenitic matrix (gray) and eutectic on the boundaries of grains (Figure 3). The eutectoid consists of two phases, in which one of the phases is close as to its composition to the matrix, and the other — has a higher iron content and less alloying elements. According to literary

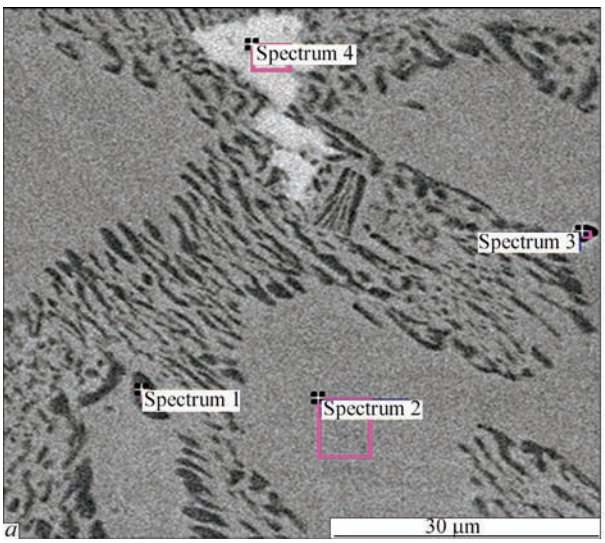


*a*

| Analysis spectrum | Element content, wt.% | | | | |
|---|---|---|---|---|---|
| | Al | Si | Cr | Mn | Fe |
| 1 | 12.61 | – | 8.06 | 33.43 | 45.91 |
| 2 | 13.62 | 0.56 | 4.76 | 24.13 | 56.93 |
| 3 | 29.63 | 0.24 | 2.88 | 14.09 | 31.88 |
| 4 | 11.51 | 0.97 | 6.92 | 30.81 | 49.78 |

*Note*. Spectrum 3 — 18.47 % N, 1.98 % O, 0.55 % Mg, 0.28 % S.

*b*

**Figure 1.** Structure of metal of investigated steel (*a*) in the cast state without etching (BEI mode) and results of local chemical analysis of specimens (*b*)

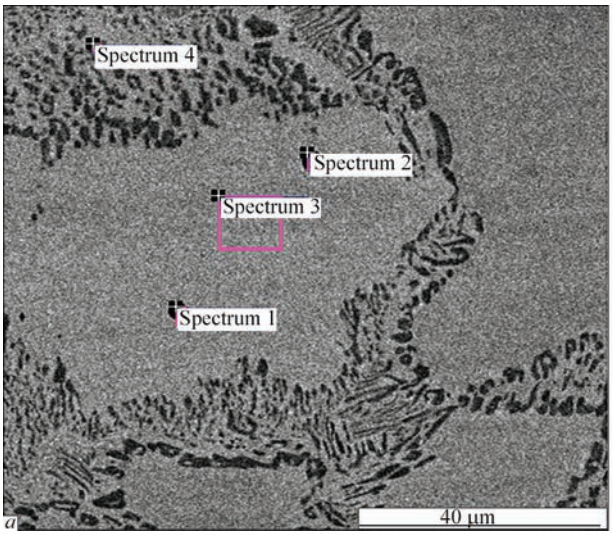


| Analysis spectrum | Element content, wt.% | | | | |
|---|---|---|---|---|---|
| | N | O | Al | Cr | Mn |
| 1 | 23.36 | 3.87 | 46.4 | 1.61 | 7.21 |
| 2 | 27.72 | 4.49 | 48.1 | 1.20 | 5.26 |
| 3 | – | – | 13.6 | 4.68 | 24.08 |
| 4 | – | – | 13.6 | 8.12 | 32.05 |

*Note*. Spectrum 1 — 0.9 % Mg, Spectrum 2 — 0.98 % Mg. Remnant — iron.

*b*

**Figure 2.** Structure of metal of investigated steel (*a*) in the cast state without etching (BEI mode) and results of local chemical analysis of NI (*b*)

sources [1, 10, 17, 19, 21], a two-phase structure can be identified as an ordered ferritic structure and κ-carbide, which is formed at a slow cooling in Fe–Mn–Al–C steels. At elevated carbon concentrations such as in Triplex steels (1.2 % C), an eutectoid reaction of austenite conversion to laminar ferrite and κ-carbide (κ-carbide is FCC carbide of (Fe, $Mn)_3A1C$) type occurs.

In order to determine how uniform alloying elements were distributed in the metal of the studied steel in the cast state after melting in the induction furnace, a linear scanning was carried out according to the selected element on the surface of the specimen. According to the linear distribution of the basic alloying elements on the surface of the specimen in the area of the formed eutectic, a decrease in iron content, an increase in the content of manganese and chromium and some reduction in aluminium content (Figure 4) were established.

As is known [22, 23, 27], the basic parameters of crystallization, which determine the dispersion of the structure, is the crystallization rate and the temperature gradient of the crystallization front. The greater the dispersion of the structure, which may be indicated by the distance between the primary or secondary branches of dendrites, the more homogeneous metal and the better its properties in the cast state and the less banding in the deformed metal. The distance between the primary and secondary branches of dendrites is a direct indicator of the dispersion of the primary structure.

The results of the study of the dendritic (primary) structure are shown in Figure 5. In the interdendritic space, a darker complex component was formed, which is revealed as a two-phase structure of acicular type at a magnification. Dendrites are oriented in different directions relative to the axis of the ingot and have the axes of the first and second order. They

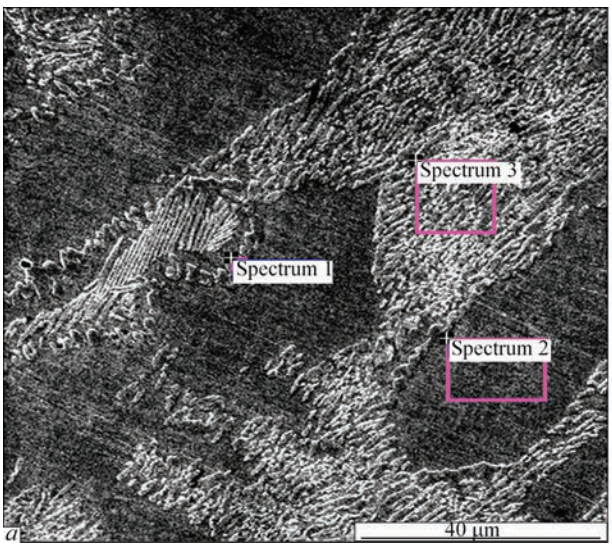


| Analysis spectrum | Element content, wt.% | | | | |
|---|---|---|---|---|---|
| | Al | Si | Cr | Mn | Fe |
| 1 | 12.98 | 0.37 | 7.12 | 29.74 | 49.78 |
| 2 | 13.75 | 0.61 | 4.64 | 24.15 | 56.85 |
| 3 | 12.51 | 0.58 | 6.72 | 28.21 | 51.98 |

*b*

**Figure 3.** Structure of metal of investigated steel (*a*) in the cast state after etching (BEI mode) and results of local chemical analysis of specimens (*b*)

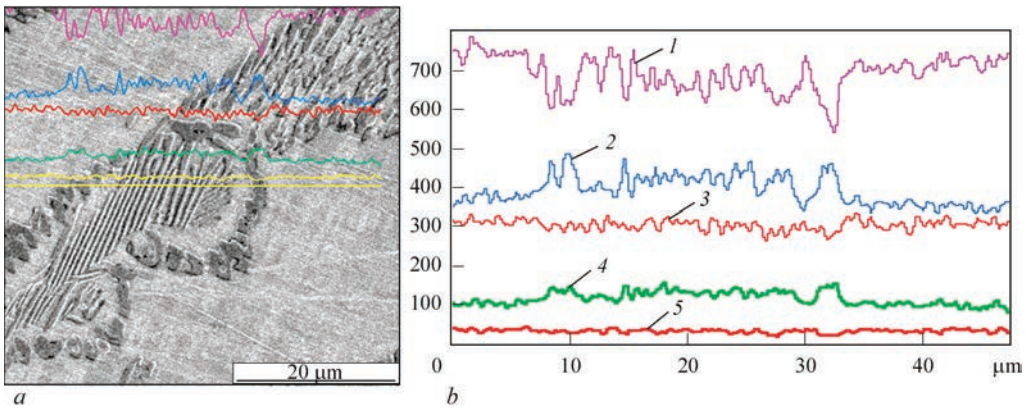


**Figure 4.** Microstructure (*a*) and linear distribution (*b*) of basic elements over the cross-section of metal specimen in the cast state: *1* — Fe; *2* — Mn; *3*—Al; *4* — Cr; *5* — Si

have an elongated shape with a length to width ratio of 5:1. The distance between the axes of the first order is 281.5–306.5 μm and 44.41–45.19 μm between the axes of the second order.

In the specimen from the area close to the surface of the ingot, the formation of branched cracks along the boundaries of the dendrites is observed, which mainly penetrate into the interdendritic space (Figure 6, *a*). Their formation can be a consequence of the liquation of alloying elements and, first of all, aluminium and manganese, which form brittle eutectics, that can be removed by remelting and appropriate heat treatment. In addition, in the specimen metal, that was taken close to the surface of the ingot, during the measurement of microhardness, cracks were formed already at a load of 50 kg/mm$^2$, which indicates an increased brittleness of the metal (Figure 6, *b*). The cracks propagated mainly along the boundaries of the dendrites.

According to the results of durometric tests, it was established that in the metal of the ingot produced by casting into a casting mould after induction melting, the dark and light phases have an increased level of microhardness (4219 ± 370 and 4405 ± 375 MPa, respectively) compared to the matrix (3220 ± 300 MPa) and two-phase areas (3219 ± 360 MPa).

## RESULTS OF METALLOGRAPHIC EXAMINATIONS OF METAL AFTER ESR

Electroslag remelting, during which there is no large volume of liquid metal that solidifies simultaneously, contributes to a more uniform distribution of alloying elements at the macrolevel during crystallization of large

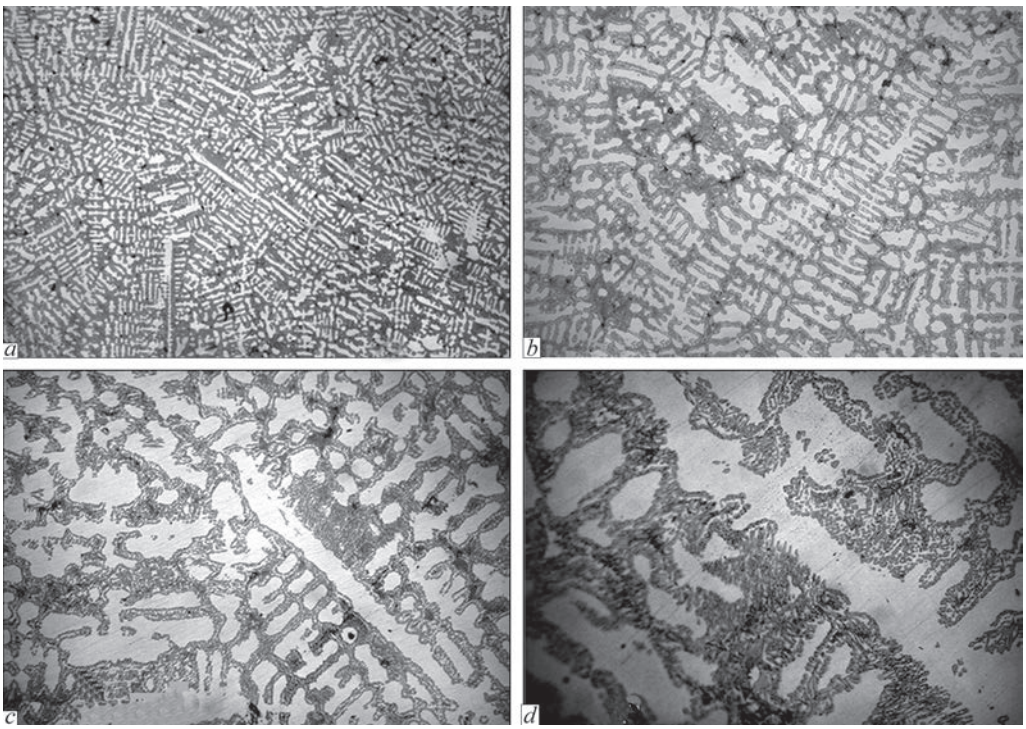


**Figure 5.** Dendritic microstructure at different magnification of characteristic areas of cast metal specimen from ingot with a diameter of 0.08 m (central part): *a* — ×50; *b* — ×100; *c* — ×200; *d* — ×400

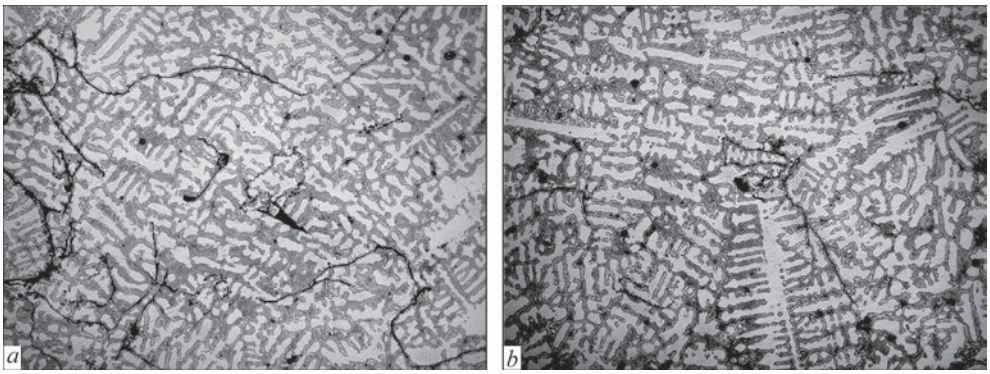

**Figure 6.** Distribution of microcracks on the areas close to the ingot surface of the cast metal (*a*) and after measurement of microhardness (*b*), ×100

ingots, and the faster growth of a dense dendritic structure suppresses the propagation of microliquations.

The study of the microstructure of the ingot metal by ESR on the specimens without etching showed that, as in the metal of cast ingots, a clear separation of the phase components in the metal structure is observed: of dark (spectrum 3) and two types of light (spectra 1, 2, 5) colour, which differ by the content of Al, Mn, Cr and Si (Figure 7).

The matrix has a light colour and contains up to: 13 wt.% Al, 1.27 wt.% Si, 5 wt.% Cr and 24 wt.% Mn. In the dark component, an increased content of such elements is observed: Mn up to 30 wt.%, Cr up to 10 wt.% (Figure 7), which is typical for the carbide phase of chromium-alloyed κ-carbide $(Fe, Mn)_3A1C$ type.

The studies have shown a uniform distribution of dispersed NI of up to 2 μm in size with a regular globular shape (Figure 7, spectra 4, 6, 7). According to their chemical composition, they represent aluminium oxynitride with magnesium impurities of up to 5.39 % (Figure 7, spectrum 7). Characteristic NI represent aluminosilicates (spectra 4, 6). The last inclusion (spectrum 7) has an extremely high content of magnesium — almost 10 %, which indicates a slag component of the inclusion.

The study of the heterogeneity of distributing alloying elements in the axes of dendrites and interdendritic space showed that the content of aluminium in the axes of dendrites is 12.05–12.85 wt.%, silicon — 1.04–1.11 wt.%, chromium — 4.88–5.06 wt.%, manganese — 23.93–24.53 wt.%, the aluminium content in the interdendritic space decreases to 10.53–10.63 wt.% and silicon to 0.85–0.92 wt.%, the content of chromium grows to 7.02–7.2 wt.% and manganese to 28.23–28.60 wt.%.

The linear distribution of the basic alloying elements on the surface of the specimen (Figure 8) along the dendrite axis and in the interaxial space confirmed the results of the local analysis. In the axes of dendrites, the content of aluminium and silicon grows and the content of chromium and manganese decreases compared to the interdendritic space.

In order to determine the features of the dendritic structure after etching of ESR metal specimens from the upper and middle parts of the ingot with a diameter of 180 mm, the primary structure of the cast metal was revealed, which consists of light-coloured

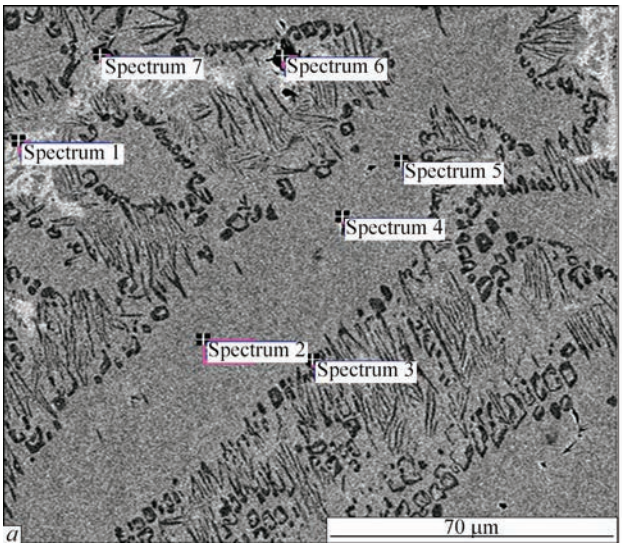


*a*

| Analysis spectrum | Element content, wt.% | | | | |
|---|---|---|---|---|---|
| | Al | Si | Cr | Mn | Fe |
| 1 | 11.40 | 0.95 | 6.50 | 28.17 | 52.98 |
| 2 | 12.72 | 1.27 | 4.75 | 23.91 | 57.34 |
| 3 | 12.90 | – | 9.29 | 35.31 | 42.50 |
| 4 | 9.82 | 5.10 | 4.25 | 21.84 | 50.95 |
| 5 | 13.30 | 1.49 | 4.79 | 23.43 | 56.99 |
| 6 | 3.43 | 2.51 | 9.98 | 14.38 | 55.47 |
| 7 | 3.94 | 1.12 | 8.74 | 29.57 | 41.39 |

*Note*. Spectrum 4 — 8.04 % O, Spectrum 6 — 8.76 % O, Spectrum 7 — 9.85 % O, 5.39 % Mg.

*b*

**Figure 7.** Structure of investigated metal (*a*) after ESR (BEI mode) and results of local chemical analysis of specimens without etching (*б*)

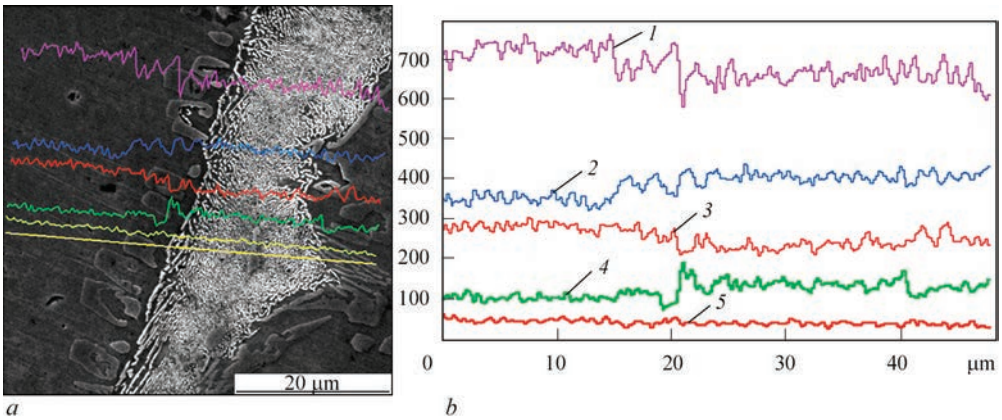


**Figure 8.** Microstructure (*a*) and linear distribution (*b*) of basic elements over the cross-section of ESR metal specimen: *1* — Fe; *2* — Mn; *3* —Al; *4* — Cr; *5* — Si (dendrite axes — dark; interdendritic space — light)

dendrites, indicating the presence of the austenitic structure, and a dark phase of the interdendritic space (Figure 9). In general, the microstructure is characterized by a homogeneous dense structure. Cracks, slag inclusions and delaminations at the boundaries of dendritic grains, unlike cast metal, are not observed. Dendrites are located in different directions relative to the axis of the ingot and have axes of the first and second order. Dendrites are smaller unlike the initial metal of the electrode (in the cast metal), have an elongated shape with a length to width ratio of 3:1. The dispersion of the dendritic structure in the ESR ingot metal was also evaluated in height. Sufficiently uniform values of the distance between the axes of the first and second order in the middle and upper parts of the ingot were established, which are respectively 136.6–146.5 and 60.54–68.92 μm.

Comparison of the metal microstructure in the specimens from the upper and middle parts of the ESR ingot showed that in the middle of the ingot in the area close to its surface, a number of dispersed nonmetallic inclusions is greater. The predominant size of the inclusions is less than 3 μm, however, single inclusions of up to 5 μm in size are observed. In terms of chemical composition, similar to the initial metal, complex inclusions of aluminium oxynitride and aluminium oxide with calcium (aluminocalcium silicates) are encountered, which can be formed as a result of interaction with slag during ESR.

It was also established that along the boundaries of dendrites axes, there are precipitations of separate

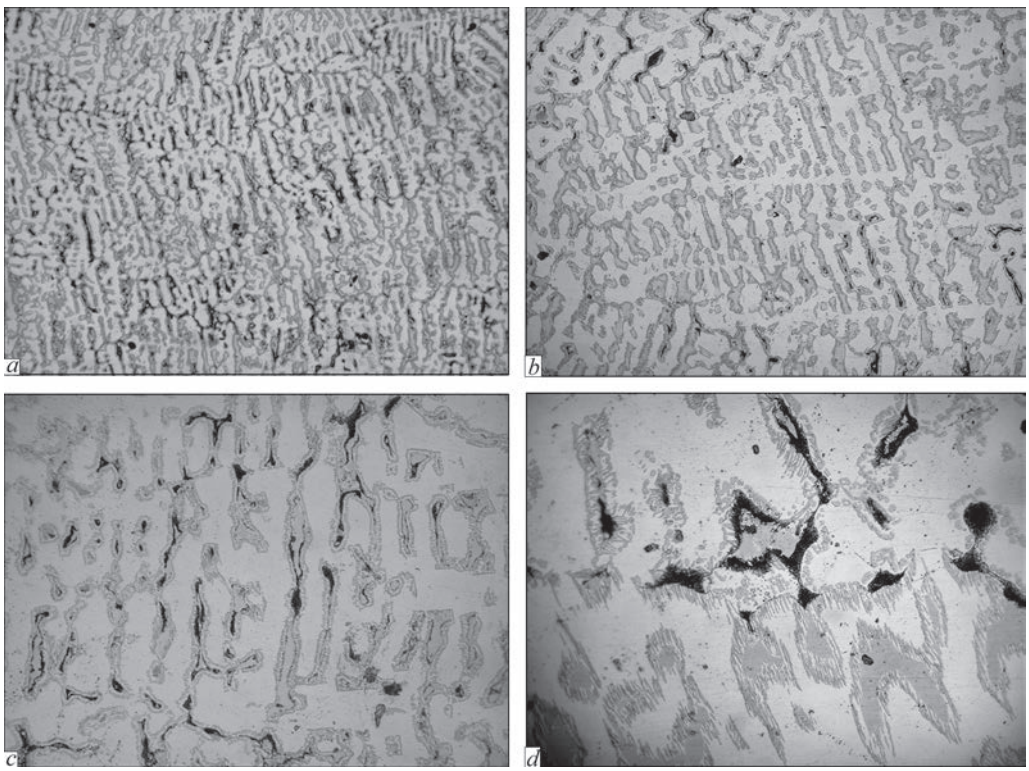


**Figure 9.** Dendritic microstructure at different magnification of characteristic areas of metal specimen from ESR ingot with a diameter of 0.18 m after etching (upper part): *a* — ×50; *b* — ×100; *c* — ×200; *d* — ×400

areas of light-coloured eutectic, which differs in the chemical composition and level of microhardness and has a reduced melting temperature, which can lead to its premature melting and a decrease in the metal properties under appropriate operating conditions. To eliminate the risk of melting, it is necessary to carry out appropriate heat treatment in order to form a more uniform distribution of alloying elements (Al, Mn, Cr) in the metal matrix. The presence of a eutectic can lead to the formation of primary cracks, as evidenced by dark regions in the middle of the eutectic.

In the upper part of the ESR ingot, as in the initial metal, in terms of the level of microhardness, the dark component and the light phase have an increased level of microhardness — 4427 ± 215 and 4386 ± 560 MPa, respectively, relative to the matrix and eutectic — 3119 ± 400 and 3208 ± 208 MPa, respectively. However, in the middle (in height) of the ingot, an increase in the level of microhardness of the dark component to 6226 ± 140, and of the light component to 4205 ± 420 MPa is observed, which may be a consequence of an uneven distribution of phases.

Evaluation of the dispersion of the dendritic structure in the metal of the ESR ingot over its height showed a sufficiently uniform distribution of the distance between the axes of the first and second order in the middle and upper parts of the ingot, which make up 136.6–146.5 and 60.54–68.92 μm, respectively.

In general, the distribution of alloying elements Al, Mn, Cr and Si, which is observed in the studied metal, is characteristic (according to literary data) for structural components of steels of this type. Obviously, in order to ensure their more uniform distribution and formation of the structure characteristic for high-strength steels, additional thermodeformational and heat treatment should be carried out, which is provided by the standard cycle of their manufacture. The excessive growth of silicon concentration in metal during ESR can be prevented by carrying out the process under the silicon-free fluxes [32].

In general, metallographic examinations showed that the microstructure of all experimental specimens is austenitic with the dendritic shape of crystals. Cracks, slag inclusions and delaminations on the boundaries of grains in the ESR ingot metal were not detected.

The carried out studies show that for steels with a high content of manganese, aluminium and carbon, the controlled conditions of solidification should be provided, at which the cooling rate, on the one hand, should be sufficiently high to form a uniform structure and, on the other, not cause cracks in thermally stressed zones.

The carried out studies have shown that electroslag remelting of cast billets of Fe–Mn–Al–C steel provides improvement of the structure and reduction of the size of nonmetallic inclusions without significant changes in the content of leading alloying components, which makes it possible to produce large-sized homogeneous ingots.

## CONCLUSIONS

1. High-strength lightweight Fe–Mn–Al–C steels are high-tech alloys, which simultaneously show excellent ductility along with high strength, as well as reduced density depending on the aluminium content. Acquiring the required level of properties by them is determined by the complex dependence between the chemical composition and the macro- and microstructures formed during the process of solidification of the alloy and during the subsequent heat and thermomechanical treatment.

2. High-alloy Fe–Mn–Al–C steels like other steels with a high content of manganese, are complex alloys for pouring, prone to hot cracking, formation of coarse structure and development of macro- and microliquation. Structural heterogeneities resulting from the segregation of impurities affect the distribution of mechanical properties, corrosion resistance, efficiency and results of heat and mechanical treatments.

3. The performed studies confirm the conclusions that for steels of this type it is necessary to thoroughly control the conditions of solidification so that, on the one hand, to minimize the segregation of impurities, and on the other, to prevent the formation of cracks in the areas of thermal stress. The obtained results illustrate the significant impact of cooling rate on crack formation, distribution of manganese and aluminium at macro- and microlevels and parameters of dendritic structure of the alloy.

4. Electroslag remelting of cast billets provided improvement of the structure and led to a decrease in the size of NI in the studied metal without significant changes in the content of leading alloying elements, which is a prerequisite for producing large-sized homogeneous ingots. Distribution of Mn, Al, Cr and Si at the microlevel according to the values of micro X-ray spectral analysis is characteristic of high-alloy Fe–Mn–Al–C steels according to literary data.

5. Metallographic examinations showed that the microstructure in all specimens of the studied steel is characteristic of cast austenitic steel with a dendritic growth of crystals. The dendritic structure in the ESR ingot is uniform, the distances between the axes of the first and second order in the middle and upper part of the ingot are 136.6–146.5 and 60.54–68.92 μm, respectively. To complete the formation of the required microstructure, it is necessary to carry out appropriate thermodeformational and heat treatment.

6. Prior to further thermomechanical treatment, it is advisable to expose the ingots of high-alloy Fe-Mn–Al–C steels to the ESR process, which provides the improvement of crystalline structure and chemical uniformity of the cast metal, which allows reaching the required level of metal homogeneity, a certain level of properties with a smaller quantity of stages, duration of thermomechanical treatment and reduction in the consumption of resources.

## REFERENCES


1. Hansoo Kim, Dong-Woo Suh, Nack J. Kim. (2013) Fe–Al–Mn–C lightweight structural alloys: A review on the microstructures and mechanical properties. *Sci. and Technol. of Advanced Materials*, 14(**1**), 11. DOI: https://doi.org/10.1088/1468-6996/14/1/014205
2. Frommeyer, G., Drewes, E.J., Engl, B. (2000) Physical and mechanical properties of iron–aluminium–(Mn, Si) lightweight steels. *Rev. Met. Paris*, 97(**10**), 1245–1253. DOI: https://doi.org/10.1051/metal:2000110
3. Shangping, Chen, Radhakanta, Rana, Arunansu, Haldar, Ranjit, Kumar Ray (2017) Current state of Fe–Mn–Al–C low density steels. *Progress in Mater. Sci.*, **89**, 345–391. DOI: https://doi.org/10.1016/j.pmatsci.2017.05.002
4. Shao-bin, Bai, Yong-an, Chen, Xin, Liu et al. (2023) Research status and development prospect of Fe–Mn–C–Al system low-density steels. *J. of Materials Research and Technology*, **25**, 1537–1559.
5. Zambrano, O.A. (2018) A general perspective of Fe–Mn–Al–C steels. *J. Mater. Sci*., 53(**20**), 14003–14062.
6. Frommeyer, G., Brüx, U. (2006) Microstructures and mechanical properties of high-strength Fe–Mn–Al–C light-weight TRIPLEX steels. *Steel Res. Int*., **77**, 627–633. DOI: https://doi.org/10.1002/srin.200606440
7. Raabe, D., Springer, H., Gutierrez-Urrutia, I. et al. (2014) Combinatorial synthesis and microstructure-property relations for low-density Fe–Mn–Al–C austenitic steels. *JOM*, **66**, 1845–1856. DOI: https://doi.org/10.1007/s11837-014-1032-x
8. Howell, R.A., Aken, D.C. (2009) A literature review of age hardening Fe–Mn–Al–C alloys. *Iron Steel Technol*., **6**, 193–212. DOI: https://scholarsmine.mst.edu/matsci_eng_facwork/1283/
9. Chen, P., Li, X., Yi, H. (2020) The κ-carbides in low-density Fe–Mn–Al–C Steels: A review on their structure, precipitation and deformation mechanism. *Metals*, 10(**8**), 1021. DOI: https://doi.org/10.3390/met10081021
10. Khaple S., Golla B.R., Prasad V.V.S. (2023) A review on the current status of Fe–Al based ferritic lightweight steel. *Defence Technology*, **26**, 1–22. DOI: https://doi.org/10.1016/j.dt.2022.11.019
11. Frommeyer, G., Drewes, E.J., Engl, B. (2000) Physical and mechanical properties of iron–aluminium–(Mn, Si) lightweight steels. *Rev. Met. Paris*, 97(**10**), 1245–1253. DOI: https://doi.org/10.1051/metal:2000110
12. Frommeyer, G., Jiménez, J.A. (2005) Structural superplasticity at higher strain rates of hypereutectoid Fe–5.5Al–1Sn–1Cr–1.3C steel. *Metall. and Mater. Transact. A*, **36**, 295–300. DOI: https://doi.org/10.1007/s11661-005-0302-1
13. Chen, P., Xiong, X.C., Wang, G.D., Yi, H.L. (2016) The origin of the brittleness of high aluminum pearlite and the method for improving ductility. *Scr. Mater*., **124**, 42–46. DOI: https://doi.org/10.1016/j.scriptamat.2016.06.031
14. Liu, D., Cai, M., Ding, H., Han, D. (2018) Control of inter/intra-granular κ-carbides and its influence on overall mechanical properties of a Fe–11Mn–10Al–1.25C low density steel. *Mater. Sci. Eng. A*, **715**, 25–32. DOI: https://doi.org/10.1016/j.msea.2017.12.102
15. Frommeyer, G., Brüx, U., Neumann P. (2003) Supra-ductile and high-strength manganese-TRIP/TWIP steels for high energy absorption purposes. *ISIJ Int.*, **43**, 438–346.
16. Gutierrez-Urrutia, I., Raabe, D. (2013) Influence of Al content and precipitation state on the mechanical behaviour of austenitic high-Mn low-density steels. *Scripta Mater.*, **68**, 343-347.
17. Gutierrez-Urrutia, I. (2021) Low density Fe–Mn–Al–C steels: phase structures, mechanisms and properties. *ISIJ Int.*, 61(**1**), 16–25.
18. Ding, H., Li, H., Misra, R.D.K. et al. (2017) Strengthening mechanisms in low density Fe–26Mn–*x*Al–1C steels. *Steel Research Int*., **89**, 1700381. DOI: https://doi.org/10.1002/srin.201700381
19. Kim, K.-W., Park, S.-J., Moon, J. et al. (2020) Characterization of microstructural evolution in austenitic Fe–Mn–Al–C lightweight steels with Cr content. *Materials Characterization*, **170**, 110717. DOI: https://doi.org/10.1016/j.matchar.2020.110717
20. Zhuang, C. Liu, J. Li, C., Tang, D. (2019) Study on high temperature solidification behavior and crack sensitivity of Fe–Mn–C–Al twip steel. *Scientific Reports*, 9(**1**), 15962–15977.
21. Lan, P. Tang, H., Zhang, J. (2016) Solidification microstructure, segregation, and shrinkage of Fe–Mn–C twinning-induced plasticity steel by simulation and experiment. *Metallurg. and Mater. Transact. A*, 47(**6**), 2964–2984.
22. Shen, Y. Liu, J. Yang, S. et al. (2019) Dendrite growth behavior in directionally solidified Fe–C–Mn–Al alloys. *J. of Crystal Growth*, **511**, 118–126.
23. Lee, C.-Y., Lee, Y.-K. (2014) The solidification mode of Fe–Mn–Al–C lightweight steel. *JOM*, 66(**9**), 1794–1799.
24. Yaozu Shen, Shufeng Yang, Jianhua Liu et al. (2019) Study on micro segregation of high alloy Fe–Mn–C–Al steel. *Steel Research Int*., **90**, 1800546. DOI: https://doi.org/10.1002/srin.201800546
25. Grajcar, A., Kaminska, M., Opiela, M. et al. (2012) Segregation of alloying elements in thermomechanically rolled medium-Mn multiphase steels. *Mater. Manuf. Eng*., 55(**2**), 256–264.
26. Wietbrock, B., Bambach, M., Seuren, S., Hirt, G. (2010) Homogenization strategy and material characterization of high-manganese TRIP and TWIP steels. *Mater. Sci. Forum*, **638–642**, 3134–3139. DOI: https://doi.org/10.4028/www.scientific.net/msf. 638-642. 3134.
27. Senk, H. Emmerich, J. Rezende, R. Siquieri D. (2007) Estimation of segregation in iron-manganese steels. *Advanced Engineering Materials*, **8**, 695–702. DOI: 10.1002/adem.200700138
28. Shen, Y. Yang, S. Liu et al. (2019) Study on micro segregation of high alloy Fe–Mn–C–Al steel. *Steel Research Int.*, 90(**5**), 2963–2975. DOI: https://doi.org/10.1002/srin.201800546
29. Jan Reitz, Burkhard Wietbrock, Silvia Richter et al. (2011) Enhanced homogenization strategy by electroslag remelting of high-manganese TRIP and TWIP steels. *Advanced Engineering Materials*, 13(**5**), 395–399. DOI: 10.1002/adem.201000322
30. Kang-Wei LI, Chang-Ling ZHUANG, Jian-Hua LIU et al. (2015) Smelting and casting technologies of Fe–25Mn–3Al–3Si twinning induced plasticity steel for automobiles. *J. of Iron and Steel Research Int.*, **22** (Supplement 1), 75–79. DOI: https://doi.org/10.1016/S1006-706X(15)30142-4
31. Sa Ge, Mihaiela Isac, Roderick Ian Lawrence Guthrie (2013) Progress in strip casting technologies for steel; technical developments. *ISIJ Int.*, 53(**5**), 729–742. DOI: https://doi.org/10.2355/isijinternational.53.729

32. Medovar, L., Stovpchenko G., Lisova, L. et al. (2023) Features and restrictions of electroslag remelting with silica-bearing slags for lightweight high manganese steel. *Steel Research Int*., 94(**10**), 202300161. DOI: https://doi.org/10.1002/srin.202300161

**ORCID**
Yu.V. Kostetskyi: 0000-0003-0742-0684,
G.O. Polishko: 0000-0001-7543-280X,
V.A. Kostin: 0000-0002-2677-4667,
V.P. Petrenko: 0000-0003-2440-1901,
E.O. Pedchenko: 0000-0002-8824-4389

**CONFLICT OF INTEREST**
The Authors declare no conflict of interest

**CORRESPONDING AUTHOR**
Yu.V. Kostetskyi
E.O. Paton Electric Welding Institute of the NASU
11 Kazymyr Malevych Str., 03150, Kyiv, Ukraine.
E-mail: y.kostetsky@paton.kiev.ua

**SUGGESTED CITATION**
V.A. Zaitsev, Yu.V. Kostetskyi, G.O. Polishko, V.A. Kostin, V.P. Petrenko, E.O. Pedchenko (2023) Investigations of the quality of metal of high-manganese steel alloyed by aluminium and chromium after electroslag remelting. *The Paton Welding J*., **12**, 39–49.

**JOURNAL HOME PAGE**
https://patonpublishinghouse.com/eng/journals/tpwj

Received: 05.09.2023
Accepted: 26.12.2023

## NEW BOOK


Igor Ryabtsev, Serhii Fomichov, Valerii Kuznetsov, Yevgenia Chvertko, Anna Banin
**Surfacing and Additive Technologies in Welded Fabrication**
Springer Nature Switzerland AG 2023, 226 p.
ISBN 978-3-031-34389-6, ISBN 978-3-031-34390-2 (eBook)
https://doi.org/10.1007/978-3-031-34390-2

This book provides a comprehensive overview of a wide range of surfacing methods, detailing their physical basics and technologies.

Each section of the book provides information on the formation of the structure and properties of the deposited metal, the reasons for the formation of defects, and directions for prevention. The book also covers the certification of surfacing procedures, adhering to international standards.

With a focus on practical applications, the book is an essential reference for anyone working in the field of welding and related technologies. It includes detailed illustrations and diagrams, making it easy to understand and follow the concepts.

**CONTENTS**